Extended Data

Lymph node-targeted Nanovaccine Reshapes the Tumor Microenvironment to Suppress PDAC Progression and Metastasis

Ron Kleiner[1§], Daniella Vaskovich-Koubi[1§], Yair Roth[1], Adan Miari[1], Sagi Gordon[2], Rita C. Acúrcio[3], Bárbara Carreira[3], Reham Abu Ghoush[4], Malak Abo Alhija[4], Katherine Margulis[4], Shelly Loewenstein[5], Lior Orbach[2,5], Guy Lahat[2,5], Dov Hershkovitz[2,6], María J. Vicent[7,8], Helena F. Florindo[3#], and Ronit Satchi-Fainaro[1,9#]

[1] *Department of Cancer Biology and Immunology, Gray School of Medical Sciences, Gray Faculty of Medical and Health Sciences, Tel Aviv University, Tel Aviv 6997801, Israel.*

[2] *Gray School of Medicine, Gray Faculty of Medical and Health Sciences, Tel Aviv University, Tel Aviv 6997801, Israel.*

[3] *Research Institute for Medicines (iMed.ULisboa), Faculdade de Farmácia, Universidade de Lisboa, Lisbon 1649-003, Portugal.*

[4] *Institute for Drug Research, School of Pharmacy, Faculty of Medicine, Center for Nanoscience and Nanotechnology, The Hebrew University of Jerusalem, Jerusalem, 9112001, Israel.*

[5] *Department of General Surgery, Tel Aviv Sourasky Medical Center, Tel Aviv 6423906, Israel.*

[6] *Department of Pathology, Tel Aviv Sourasky Medical Center, Tel Aviv 6423906, Israel.*

[7] *Polymer Therapeutics Lab, Príncipe Felipe Research Center, Valencia E-46012, Spain.*

[8] *CIBERONC, IISCIII, Madrid, Spain.*

[9] *Sagol School of Neuroscience, Tel Aviv University, Tel Aviv 6997801, Israel.*

§ *Equal contribution.*

Co-corresponding authors.

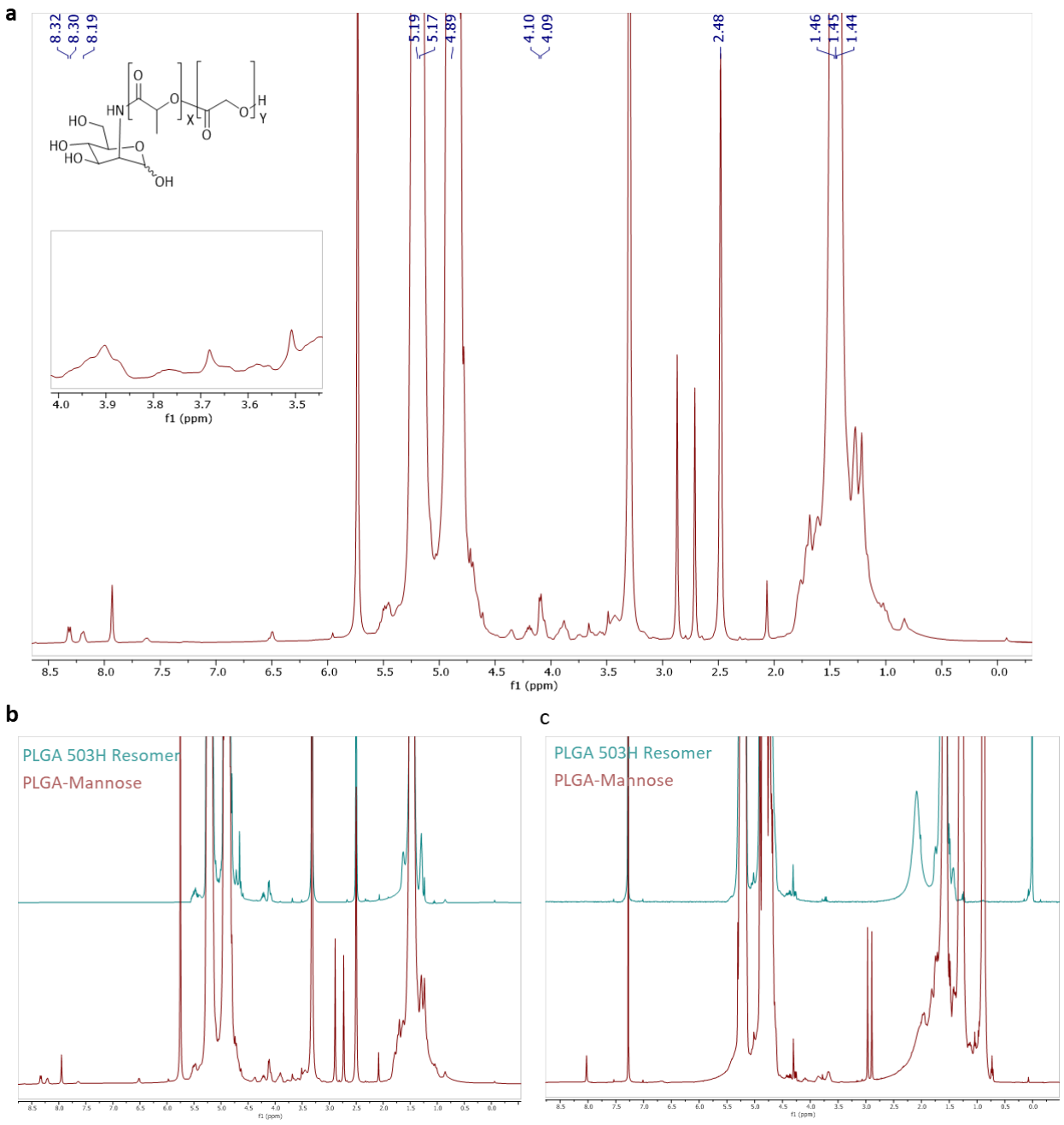

Extended Data Fig. 1| a, Hydrogen Nuclear Magnetic Resonance (H-NMR) histograms of PLGA-mannose in DMSO-d6 and PLGA-mannose structure. **b-c,** H-NMR comparison between PLGA 503H Resomer to the conjugant PLGA-mannose in **b,** DMSO-d6, and **c,** CDCl3.

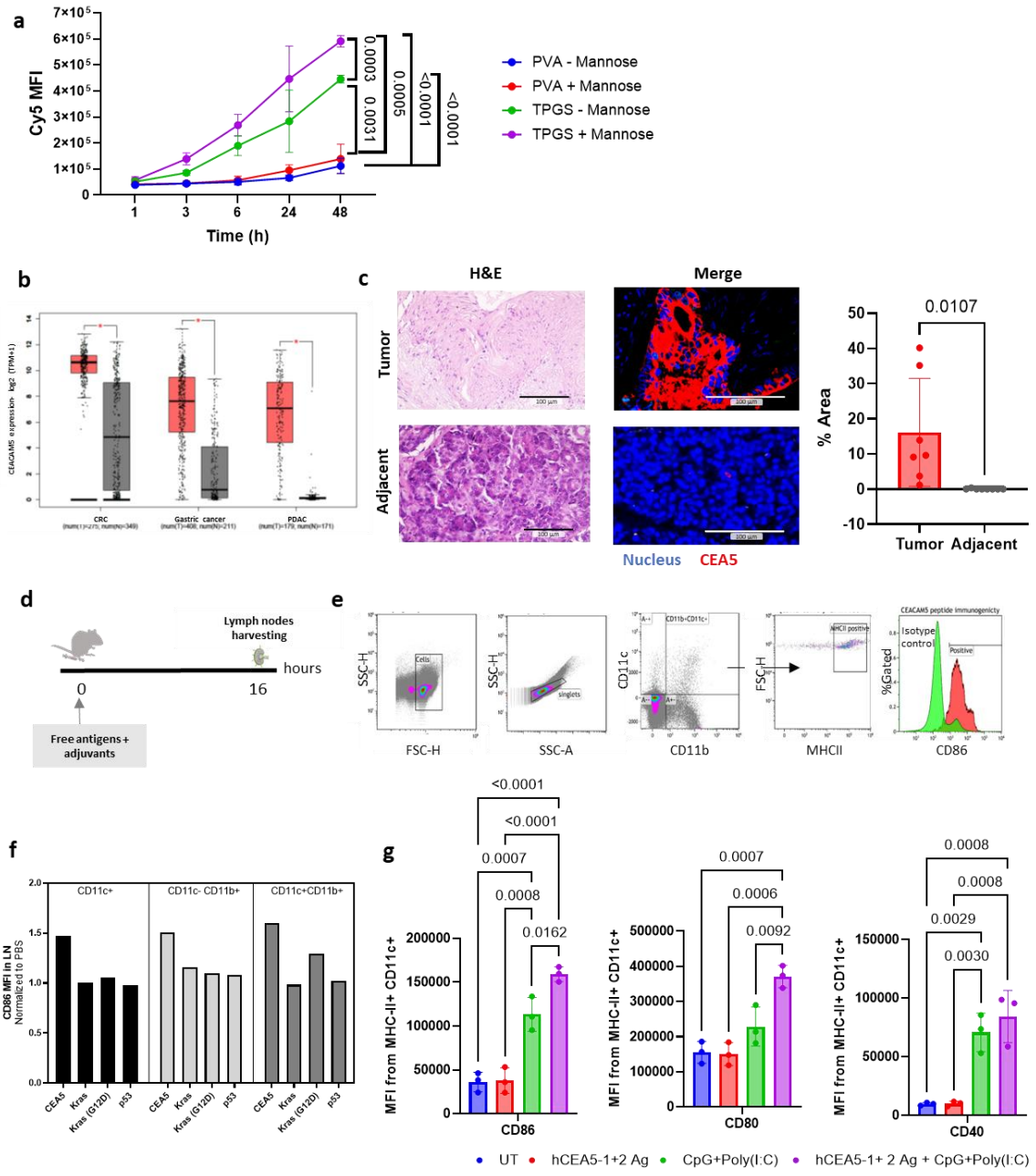

Extended Data Fig. 2| a, 4 different Cy5-labeled NPs formulations were made and incubated with bone marrow-derived dendritic cells (BMDCs) for 3, 6, 24, and 48 h. The NPs' internalization into BMDCs was measured using flow cytometry. The plot shows the mean ± SD (N = 4) with a Two-Way ANOVA. p-values presented for the 48 h time point. **b,** CEA5 expression in GI malignancies (red) compared to normal tissue (gray), the analysis was made by GEPIA2, data were obtained from TCGA and GTEx cohorts. Statistical significance was calculated using Student's t-test (all comparisons $P < 10^{-70}$). **c,** H&E and immunofluorescence (IF) images of sequential slides of PDAC patient FFPE samples. Nuclei stained by Hoechst (blue) and CEACCAM5 stained by anti-CD66e antibody (red). H&E staining was performed using a 20x magnification, and the IF staining was performed using a 40x magnification. Scale bars represent 100 µm. Quantification of the CEA5 staining represented as % area by ImageJ, N = 9 PDAC patients, Data represent mean ± SD, unpaired t-test. **d-f**, Antigen selection. **d,** Mice were injected s.c. with a mixture of free antigens and adjuvants (antigens- 100 µg, CpG- 20 µg, Poly I:C- 40 µg). I-LN nodes were isolated 16 h post-treatment. Using flow cytometry, CD86 intensity was measured as an indicator for early APC activation. **e,** Gating strategy. **f,** A comparison between the CD86 MFI levels following the different treatment groups. The data represent a pool of 3 mice/group. **g,** BMDC were incubated for 48 h with the different components of the NV free in solution (mot encapsulated in a NP): UT, hCEA5-1 and 2 Ags, CpG + Poly(I:C), or all components (CpG + Poly(I:C) + hCEA5-1 and 2 Ags). The expression of the activation markers CD86, CD80, and CD40 was ensured by flow cytometry. Data represent mean ± SD, N = 3, One-way ANOVA.

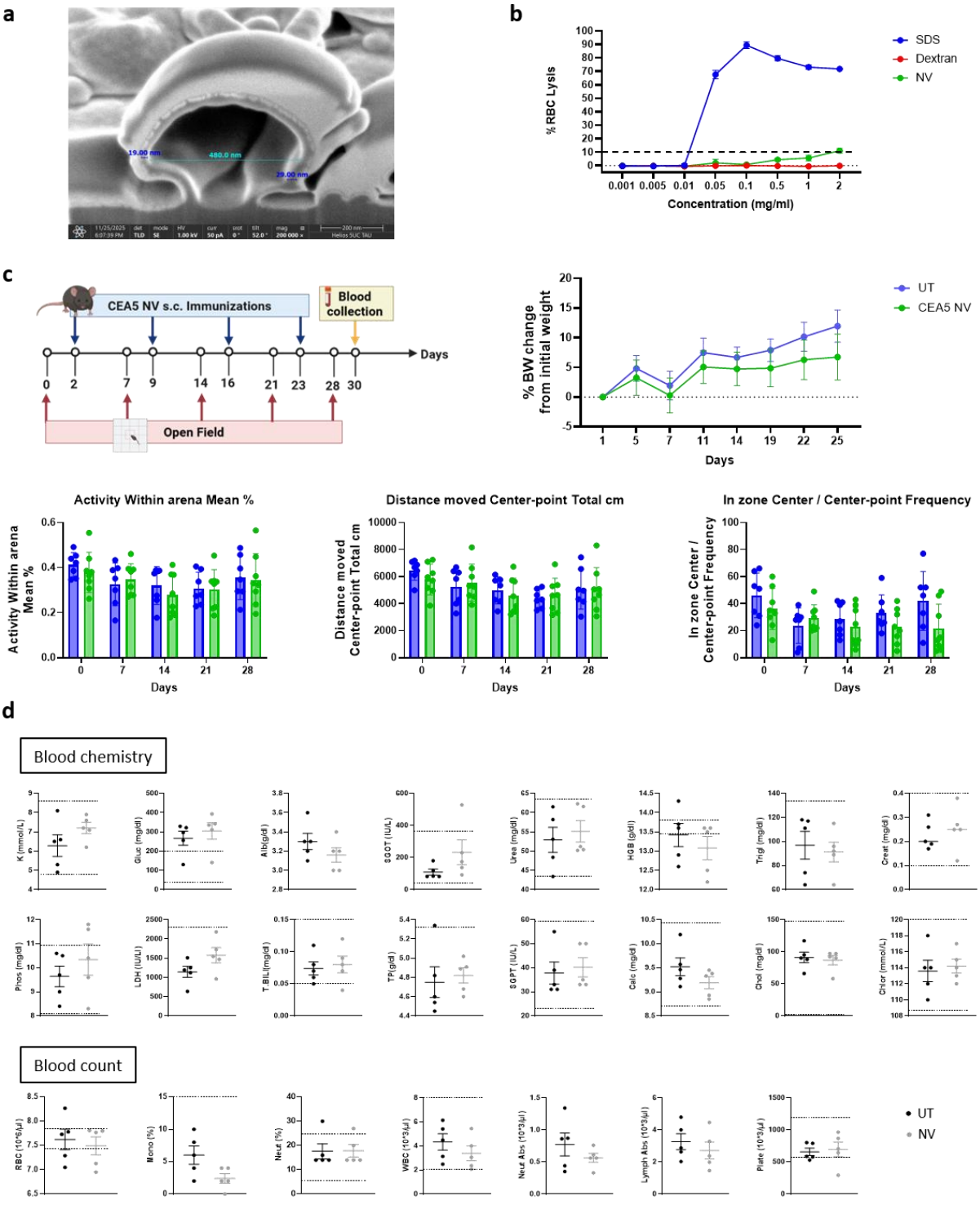

Extended Data Fig. 3| a, FIB-SEM image of 500 nm, representing 2-3% of the NV population, showing the cortex (480 nm) and core (average of 25 nm) measurements. Scale bar = 200 nm. **b,** Red blood cells were incubated with serial dilutions of NV, dextran (negative control), or sodium dodecyl sulfate (SDS, positive control) for 1 h; after that, the released percentage of hemoglobin was measured spectrophotometrically. % RBC lysis was calculated as the percentage of RBC lysis induced by Triton-X. Data are represented as mean ± SD, N = 3. **c-d,** In vivo safety. **c,** Assessment of the open field test. The distance traveled, time spent in the center of the arena, and % activity by C57BL/6 male mice during a 15-minute video recording were analyzed using EthoVision 13XT software. Data represent mean ± s.e.m., N = 8 mice. All group comparisons were NS by the One-way ANOVA test. Created with BioRender.com. **d,** Blood test (chemistry and hematology panels), N = 5 mice. All comparisons between the groups were NS by the One-way ANOVA test. Data represent mean ± s.e.m. Whisker charts show minimum and maximum values.

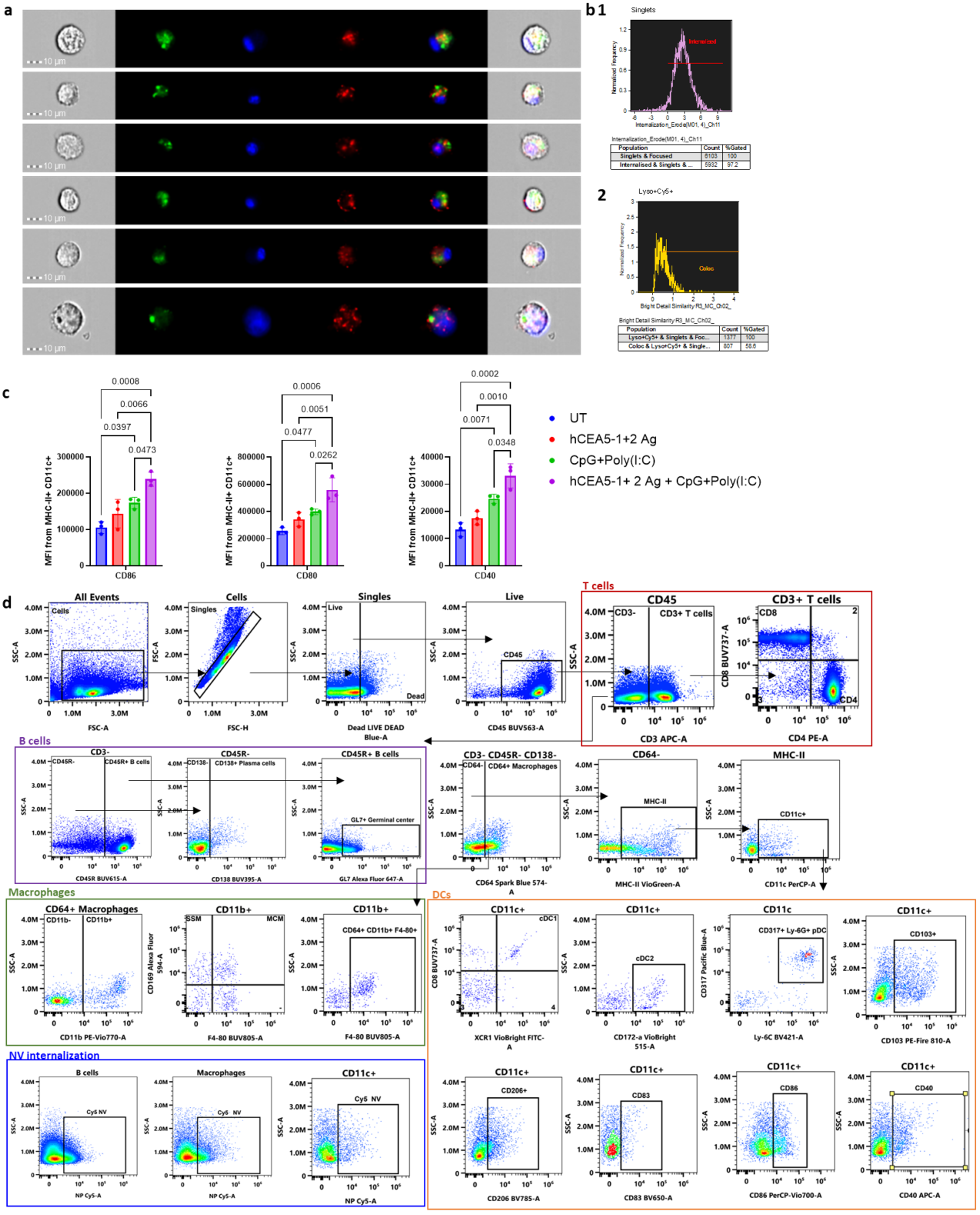

Extended Data Fig. 4| a, Image stream images and analysis of Cy5-labeled NV internalization into BMDCs and co-localization with lysotracker. **b,** Internalization and colocalization (coloc) gating. **c,** BMDC were incubated for 48 h with Empty NP, only hCEA5-1 and 2 peptides NP, only CpG + Poly(I:C) NP, or all components (CpG + Poly(I:C) + hCEA5-1 and 2 peptides) NV. The expression of the activation markers CD86, CD80, and CD40 was ensured by flow cytometry. Data represent mean ± SD, N=3, One-way ANOVA. **d,** Gating strategy for LN cell populations.

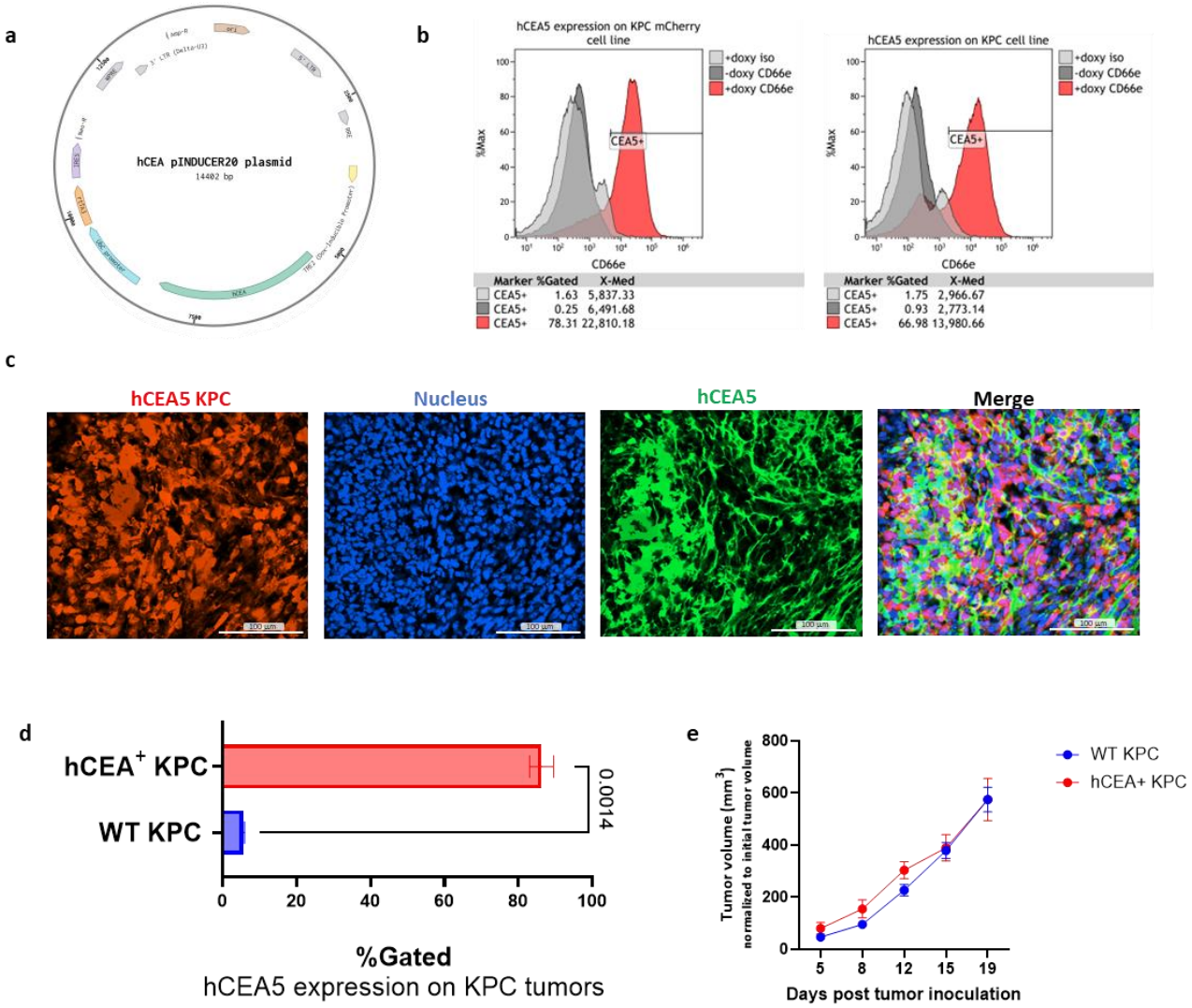

Extended Data Fig. 5| a, Schematic illustration of the lentiviral vector (14,402 bp) for doxy-inducible hCEA5 expression. The vector contains: (i) a doxy-responsive cassette featuring a TRE2 promoter driving human *CEACAM5* (hCEA); and (ii) a constitutive cassette where the UbC promoter drives a bicistronic rtTA3-IRES-NeoR transcript. Key regulatory elements (LTRs, WPRE) and bacterial selection markers (*AmpR*, *ori*) are indicated. **b,** Flow cytometry analysis of hCEA5 expression on mCherry-labeled and unlabeled KPC cells cultured in the presence of doxy and stained with anti-human CD66e Ab. Controls included doxy-treated cells stained with isotype antibody (iso) and non-induced cells (−doxy) stained with anti-human CD66e Ab. **c,** CEA5 immunostaining of mCherry-labeled hCEACEM5 KPC tumor isolated from C57BL/6 mice on day 23 following inoculation. Scale bars represent 100 µm**. d,** Flow cytometry analysis of hCEA5 expression on wild-type (WT) and CEA5^{+} KPC orthotopic tumors isolated from mice 11 days post accumulation. Data represented as mean + SD, N = 3. **e,** Tumor growth curves of orthotopic KPC and hCEA+ KPC were monitored by MRI once a week. Note that mice in both groups developed tumors and showed similar growth rates in the first week. Statistics: Two-way ANOVA, Data represent mean ± s.e.m, N = 9 mice /group.

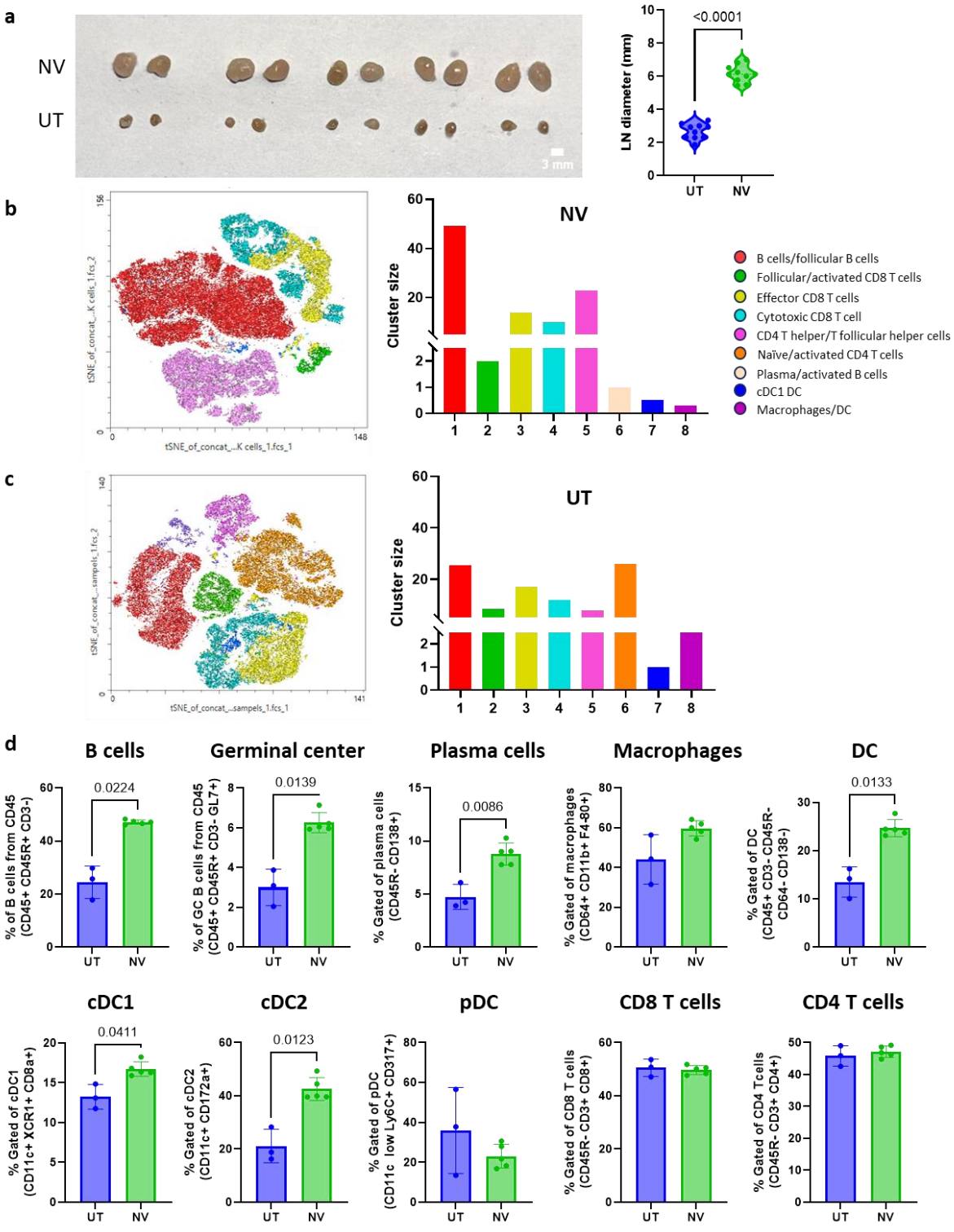

Extended Data Fig.6| I-LN were isolated from mice (two I-LN/mouse) treated 3 times with NV and from UT mice. Their size and cell populations were evaluated. **a,** representative pictures of the isolated I-LN, N = 5 mice/group (scale bar = 3 mm), and quantification of the LN's diameter presented as a violin plot, t-test. **b-c,** t-SNE visualization of FlowSOM clustering and cluster size of I-LN cell populations ($CD45^+$) isolated from UT and NV mice. Concatenated flow cytometry (N = 4) data reduced into 2D using t-SNE based on the indicated marker panel. Each dot represents a single cell and is colored according to cluster assignment. Data was acquired by spectral flow cytometry. **b**, NV N = 5. **c**, UT N = 3**. d,** The effect of NV treatment on different resident LN cells. Comparison between UT (N = 3) and NV-treated (N = 5) mice. Data represent mean ± SD, t-test.

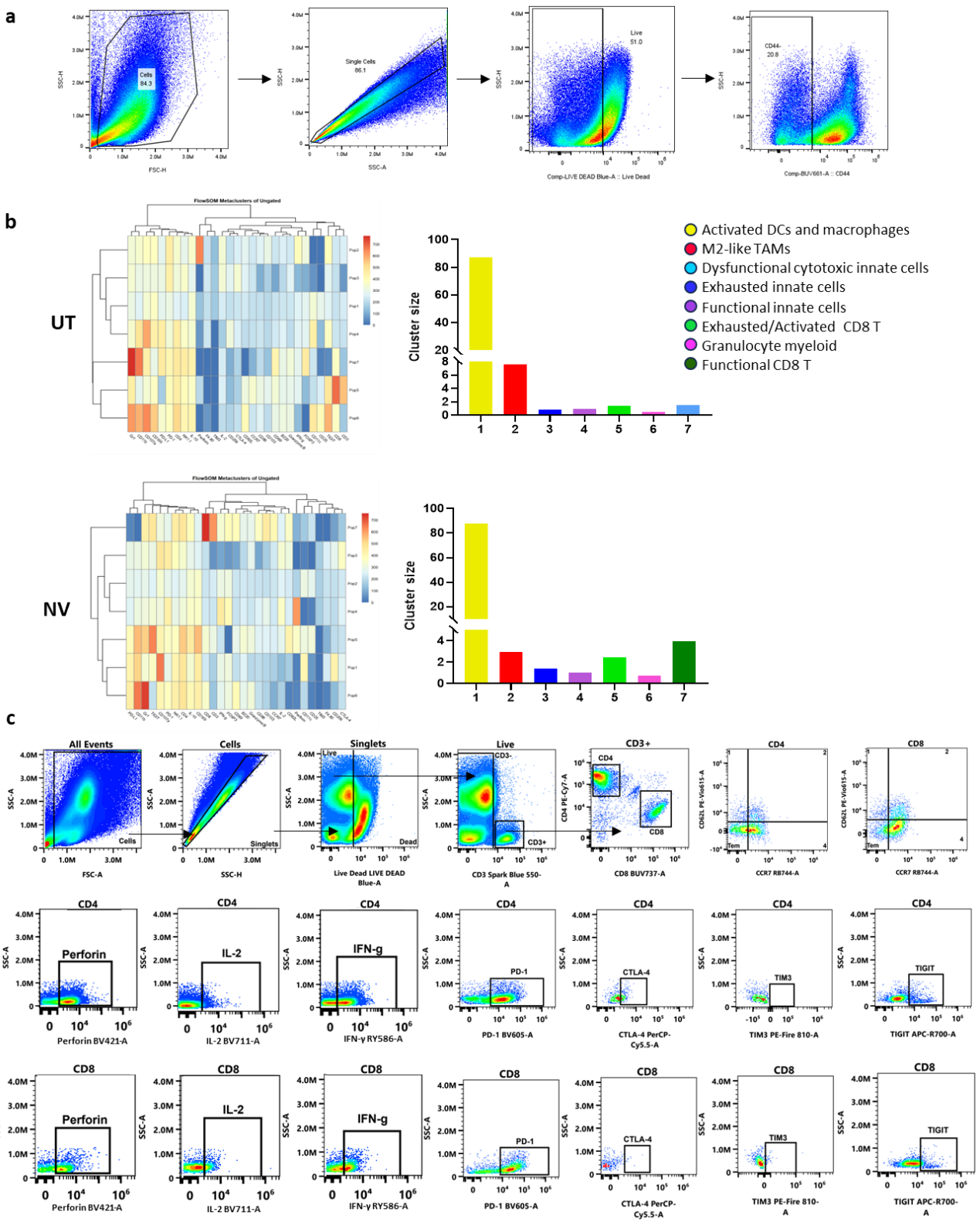

Extended Data Fig. 7| a, Gaiting strategy for t-SNE and cluster analysis. **b,** Cluster size and heatmap displaying the relative size of each population and median marker expression for FlowSOM-defined clusters (respectively) identified in UT and NV tumor samples. Rows represent clusters and columns represent the indicated immune markers. Color intensity corresponds to relative expression levels (blue, low; red, high). Clusters were annotated based on canonical lineage and functional marker expression. Cells were pre-gated for the live cell population, $CD44^-$ (KPC cell marker), and $CD45^+$. **c,** Gating strategy of activation and exhaustion markers expressed on tumor-infiltrating T cells.

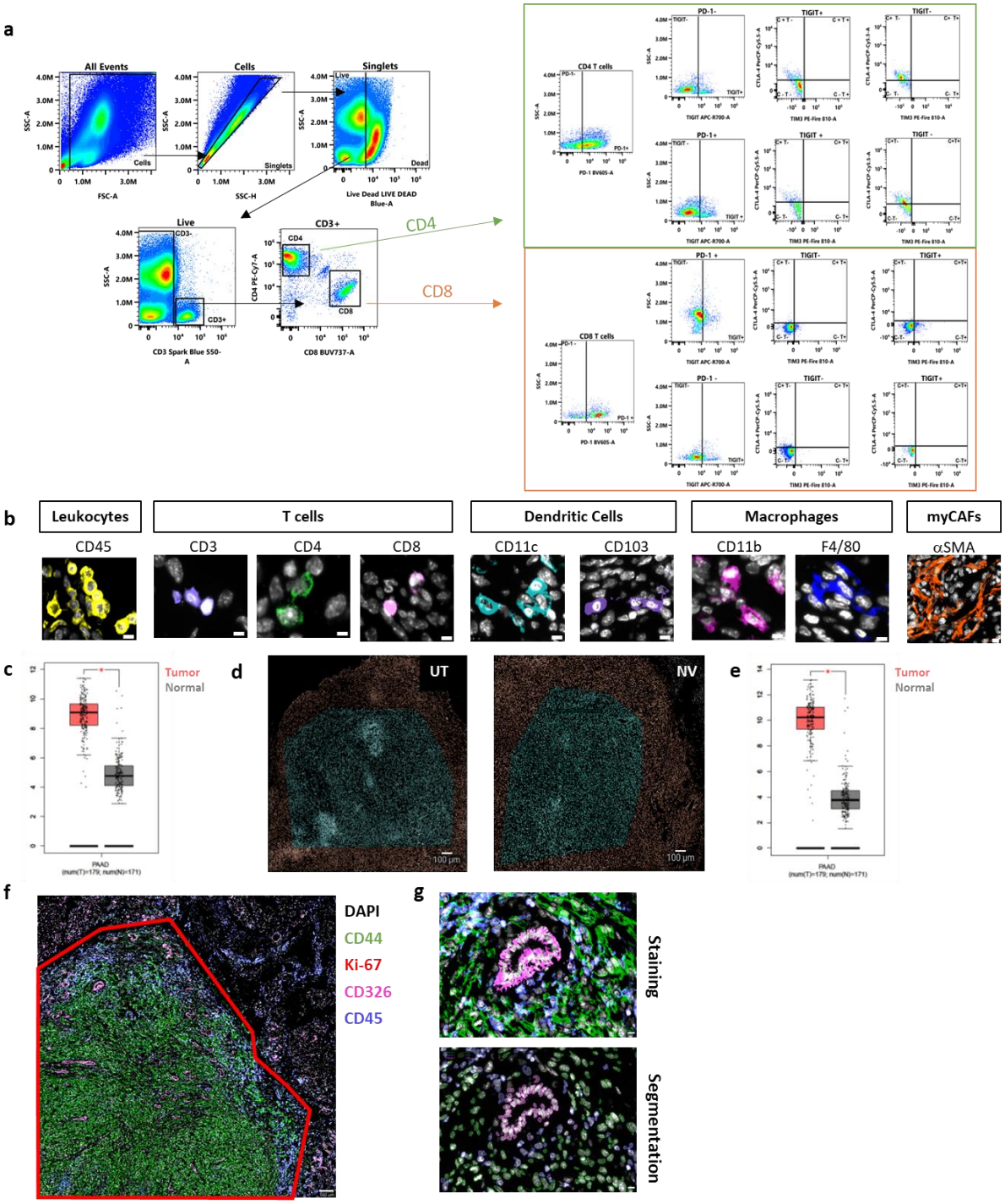

Extended Data Fig. 8| a, Gating strategy of co-expression of exhaustion markers on tumor-infiltrating T cells. **b,** Representative images for the staining performed for the segmentation shown in Fig. 2i. Scale bar = 10 µm. **c,** ACTA2/αSMA expression in PDAC malignancies (red) compared to normal tissue (gray), the analysis was made by GEPIA2, data was obtained from TCGA and GTEx cohorts. Statistical significance was calculated using Student's t-test (all comparisons $P < 10^{-70}$). **d,** ROI and segmentation used for the quantification shown in Fig. 3f. The tumor region was divided into the tumor edge (orange) and the core (cayenne). Scale bar = 100 µm. Segmentation was performed using MacsIQ View. **f-g**, ROI and segmentation used for the quantification shown in fig 4c. **e,** Col1a1 expression in PDAC malignancies (red) compared to normal tissue (gray), the analysis was made by GEPIA2, data was obtained from TCGA and GTEx cohorts. Statistical significance was calculated using Student's t-test (all comparisons $P < 10^{-70}$). **f**, ROI- Red polygon. DAPI- white, CD44- green, CD326- pink, and CD45- blue. Scale bar = 100 µm. **g,** Side-by-side comparison of the staining and segmentation. Scale bar = 8 µm. Segmentation was performed using MacsIQ View.

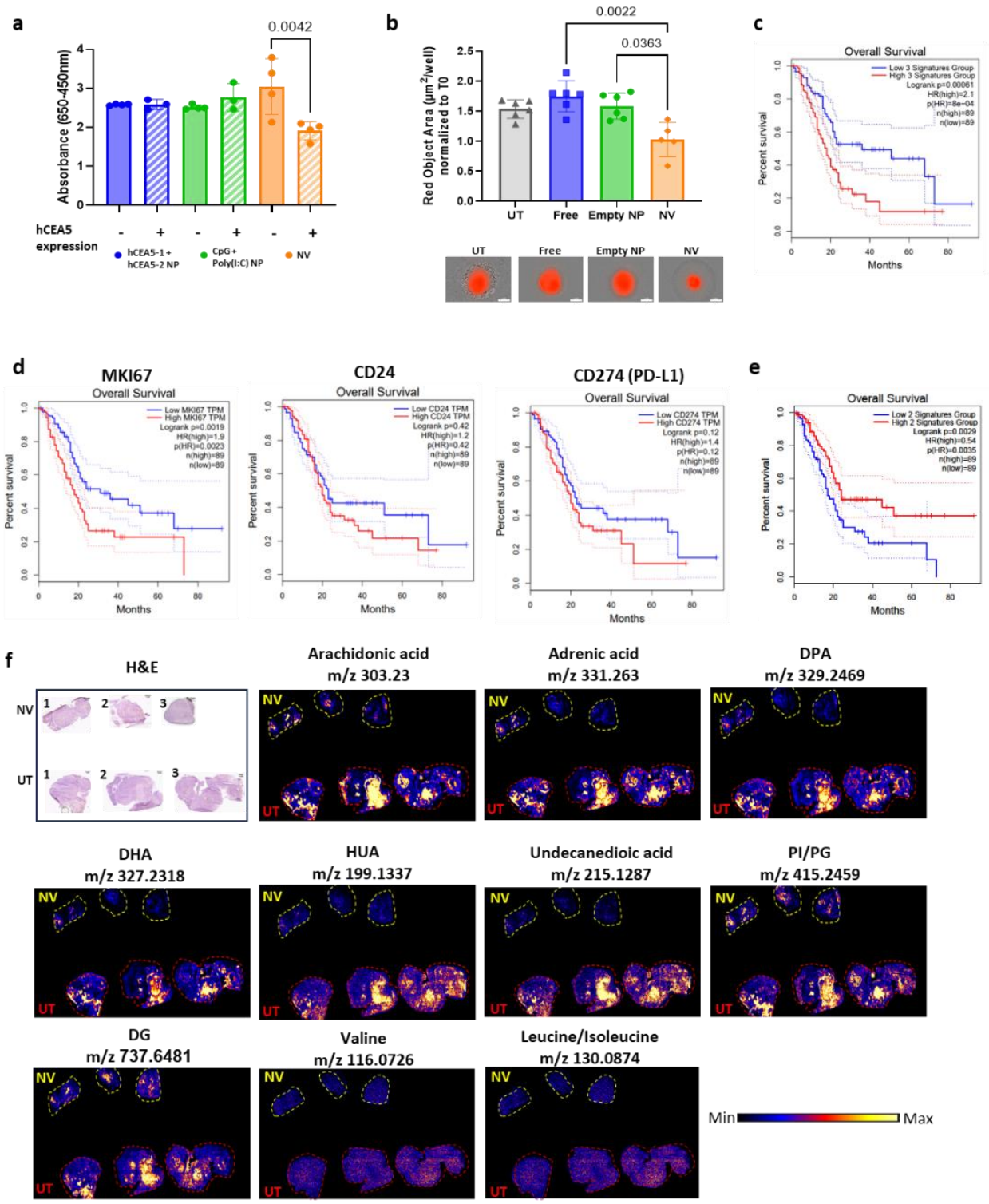

Extended Data Fig. 9| a, *Ex vivo* KPC cell killing by activated splenocytes was quantified by XTT after 72 h co-culture. KPC cells were cultured with doxycycline to induce hCEA5 expression (+) or without doxycycline, non-expressing hCEA5 (-). Mice were treated with NP containing hCEA5-1 and hCEA5-2 Ag alone, CpG+Poly(I:C) adjuvants alone, or the full NV (hCEA5-1 + hCEA5-2 + CpG + Poly(I:C)). Splenocytes were harvested 1 week after the final treatment and incubated with CEA5-1/CEA5-2 at 100 µg/mL for 24 h prior to co-culture. Data represent mean ± SD. N=3/4. Statistics: one-way ANOVA. **b,** Killing assay of hCEA5 KPC cells labeled with mCherry spheroids by activated splenocytes isolated from hCEA5 KPC bearing mice. Spheroids' growth was monitored and analyzed using Incucyte® ZOOM Live-Cell Analysis System. Graph presents the spheroid size normalized to the initial spheroid size at time 0. was, n = 5-6. Data represent mean ± SD.

Statistics: one-way ANOVA. and representative images of hCEA5 KPC 3D spheroids at 96 h, scale bar = 300 μm. **c-e**, Kaplan-Meier curves showing DFS of patients with PDAC stratified by median expression level of Ki-67, CD24, and CD274. Hazard ratio (HR), log-rank p-value, and 95% confidence intervals (dotted lines) are indicated. Data was generated using the GEPIA2 platform based on the TCGA PDAC cohort. **c,** a signature of all three genes, or **d**, each gene alone. **e**, Kaplan-Meier curves showing DFS of patients with PDAC stratified by median expression level of LARPAP1 and PGLYRP1. Hazard ratio (HR), log-rank p-value, and 95% confidence intervals (dotted lines) are indicated. Data was generated using the GEPIA2 platform based on the TCGA PDAC cohort. **f,** 2D negative ion mode DESI-MSI ion images obtained and H&E staining (scale bar = 1 mm) of NV-treated and UT hCEA^{+} KPC orthotopic PDAC tissues. m/z ions and ROI are presented. Abbreviations: Docosapentaenoic acid = DPA; Docosahexaenoic acid = DHA; Hydroxyundecenoic acid = HUA; Diacylglycerols = DG; Phosphatidylinositol = PI; Phosphatidylglycerol = PG.

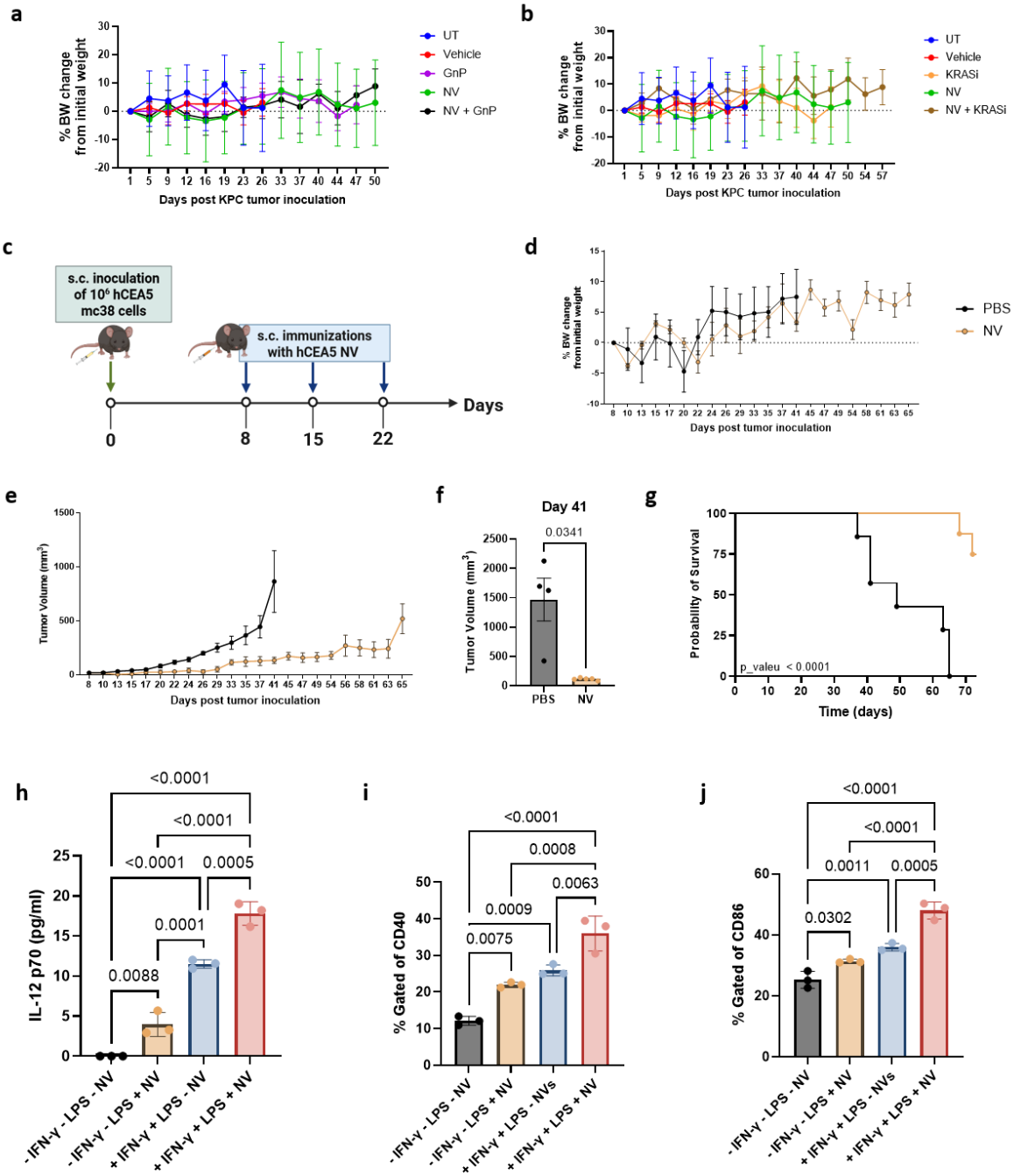

Extended Data Fig. 10| a-b, BW change follow-up of C57BL/6J mice bearing KPC tumor expressing hCEA5 treated with different treatments. **a,** UT, vehicle, NV, and GnP, GnP+NV. The graph shows the mean ± s.e.m; N = 10 mice. **b,** UT, vehicle, NV, KRASi, and KRASi+NV. The graph shows the mean ± s.e.m; N = 10 mice. **c,** Treatment schedule of hCEA5$^+$ MC38 bearing mice treated with PBS and NV, starting 8 days after tumor inoculation. Created with BioRender.com. **d,** BW change follow-up of C57BL/6J mice bearing hCEA5$^+$ MC38 tumor. **e,** Tumor growth curve. N = 7 mice/ group. **f,** Tumor volume at Day 41. Data shown as mean ± s.e.m. N = 4 (PBS), N = 5 (NV), t-test. **g,** Mice survival plot, N = 7 mice/ group. Statistics: Log-rank test. **h-j,** Activation markers of monocyte-derived DCs were measured following treatment with four conditions: PBS control (- IFN-γ - LPS - NV), NV alone (- IFN-γ - LPS + NV), IFN-γ and LPS only (+ IFN-γ + LPS - NV), or IFN-γ + LPS followed by NV (+ IFN-γ + LPS + NV). IFN-γ and LPS were added simultaneously, and 24 h later, the NV was added to the relevant groups. PBS was added to control groups at matching volumes, with one or more stimuli omitted. Data are presented as mean ± SD, N=3, t-test. **h**, IL-12p70 secretion by DC was measured by ELISA in culture supernatants collected 24 h after treatment. **i-j**, flow cytometry analysis of the DC activation markers **i**, CD40, and **j**, CD86.